ADVANCED FUNCTIONAL MATERIALS
www.afm-journal.de

Adaptive Magnetoactive Soft Composites for Modular and Reconfigurable Actuators

*Zenghao Zhang, John T. Heron, and Abdon Pena-Francesch**

Magnetoactive soft materials, typically composed of magnetic particles dispersed in a soft polymer matrix, are finding many applications in soft robotics due to their reversible and remote shape transformations under magnetic fields. To achieve complex shape transformations, anisotropic, and heterogeneous magnetization profiles must be programmed in the material. However, once programmed and assembled, magnetic soft actuators cannot be easily reconfigured, repurposed, or repaired, which limits their application, their durability, and versatility in their design. Here, magnetoactive soft composites are developed from squid-derived biopolymers and NdFeB microparticles with tunable ferromagnetic and thermomechanical properties. By leveraging reversible crosslinking nanostructures in the biopolymer matrix, a healing-assisted assembly process is developed that allows for on-demand reconfiguration and magnetic reprogramming of magnetoactive composites. This concept in multi-material modular actuators is demonstrated with programmable deformation modes, self-healing properties to recover their function after mechanical damage, and shape-memory behavior to lock in their preferred configuration and un-actuated catch states. These dynamic magnetic soft composites can enable the modular design and assembly of new types of magnetic actuators, not only eliminating device vulnerabilities through healing and repair but also by providing adaptive mechanisms to reconfigure their function on demand.

1. Introduction

Active soft materials that can be actuated by external stimuli (such as pressure, temperature, light, pH, humidity, and electrical and magnetic fields)[1,2] and generate deformation, locomotion, or mechanical work are driving the development of new robotic technologies in many applications including industrial automation, agriculture, and medical robotics.[3,4] Among these, magnetoactive soft materials are particularly interesting since they can be actuated by magnetic fields with controlled direction and intensity to generate magnetic forces and torques, thus enabling reversible and complex deformations.[1,5] Furthermore, they can be actuated remotely, without direct line of sight, and through solid objects or in confined spaces, as magnetic fields have deep media penetration without intensity attenuation. Most magnetoactive soft materials consist of a soft polymer matrix (soft elastomers and hydrogels) with dispersed micro/nanoparticles (NdFeB microparticles, superparamagnetic iron oxide nanoparticles, etc.) at specific compositions and orientations to generate alignment torques under homogeneous fields and achieve pre-programmed deformations.[5,6]

In order to achieve programmable shape-change and multimodal actuation, anisotropic magnetization profiles (i.e., inhomogeneous spatial distribution of magnetic moment) can be designed and introduced throughout the material to program torque distribution and complex deformations. Recently, several methods for programming soft ferromagnetic actuators have been developed and integrated with different design and manufacturing processes. For example, template-assisted magnetization consists of the pre-folding of magnetic composites into a predetermined shape under a saturating magnetic field, thus rewriting the magnetic domains into the field direction resulting in an anisotropic magnetization profile when unfolded.[7,8] Other methods consist in controlling the in situ orientation of the particles in an uncured polymer matrix, followed by local crosslinking to lock the particles in the desired orientation (demonstrated in 3D printing and photolithography manufacturing processes).[9–11] Other methods consist of the assembly and bonding of pre-magnetized components into modular constructs,[12,13] or in locally demagnetizing the material and remagnetizing in the desired direction.[14] Although some magnetic programming methods allow for remagnetization and reprogramming by heating above the Curie temperature and/or by exposing the sample to a high-intensity saturation field, the physical structure of magnetoactive composites is permanent as the particles are

Z. Zhang, J. T. Heron, A. Pena-Francesch
Department of Material Science and Engineering
University of Michigan
Ann Arbor, MI 48109, USA
E-mail: abdon@umich.edu
A. Pena-Francesch
Macromolecular Science and Engineering
Robotics Institute
University of Michigan
Ann Arbor, MI 48109, USA
The ORCID identification number(s) for the author(s) of this article can be found under https://doi.org/10.1002/adfm.202215248.

© 2023 The Authors. Advanced Functional Materials published by Wiley-VCH GmbH. This is an open access article under the terms of the Creative Commons Attribution License, which permits use, distribution and reproduction in any medium, provided the original work is properly cited.

DOI: 10.1002/adfm.202215248

embedded in a permanently bonded polymer network. This fundamentally reduces the design space of soft magnetic actuators and limits their reusability and their reconfigurability to adapt to new performance requirements on demand. Furthermore, due to the inherent softness of the polymer matrix, soft actuators are prone to mechanical damage (cuts, wear, tear, etc.) and to fabrication defects that typically deteriorate their physical integrity and lead to loss of properties and function. These vulnerabilities, combined with the lack of versatility and adaptability, often lead to the premature disposal of soft actuators and devices, as they cannot be easily modified, repaired, or reused. To fill this performance need, the development of soft magnetic composite materials that allow for reversible modular design and assembly is required to enable physical reconfiguration and repair on the fly.[15]

Self-healing soft materials present unique dynamic properties with opportunities to enable modular assembly, repair, and on-the-fly reconfiguration in soft actuators. Particularly, dynamic polymer networks with intrinsic healing are attractive for this, as they can reconstitute their structure across length scales over an unlimited number of cycles without loss of properties due to reversible crosslinking mechanisms.[16,17] Exploiting these dynamic properties, self-healing polymers have been implemented in soft robots and soft actuator designs to recover their function after mechanical damage.[18–20] However, these polymers typically exhibit slow healing kinetics (making the process impractical) and low modulus (limiting the work output and payload), which limit their application in robotic tasks. Recent research has demonstrated biopolymers derived from squids with remarkable healing properties that resolve this trade-off, achieving high post-healing strength (≈25 MPa) after extremely short healing times (≈1 s).[18] These squid-derived biopolymers are found in teethed structures located in the suction cups in arms and tentacles of squids used for prey capture and are composed of a group of structural proteins (15–60 kDa) that form a high-strength semicrystalline protein network (**Figure 1**a).[21,22] Squid sucker ring teeth (SRT) proteins are composed of segmented alanine-rich blocks that self-assemble into β-sheet nanostructures (2–3 nm in size) stabilized by hydrogen bonding.[23,24] These nanocrystals act as reversible physical crosslinks that enable the healing properties of the protein network, as they can be reformed after disassembling.[18] Complementing the alanine-rich blocks, glycine-rich segments connect the β-sheet nanocrystals within

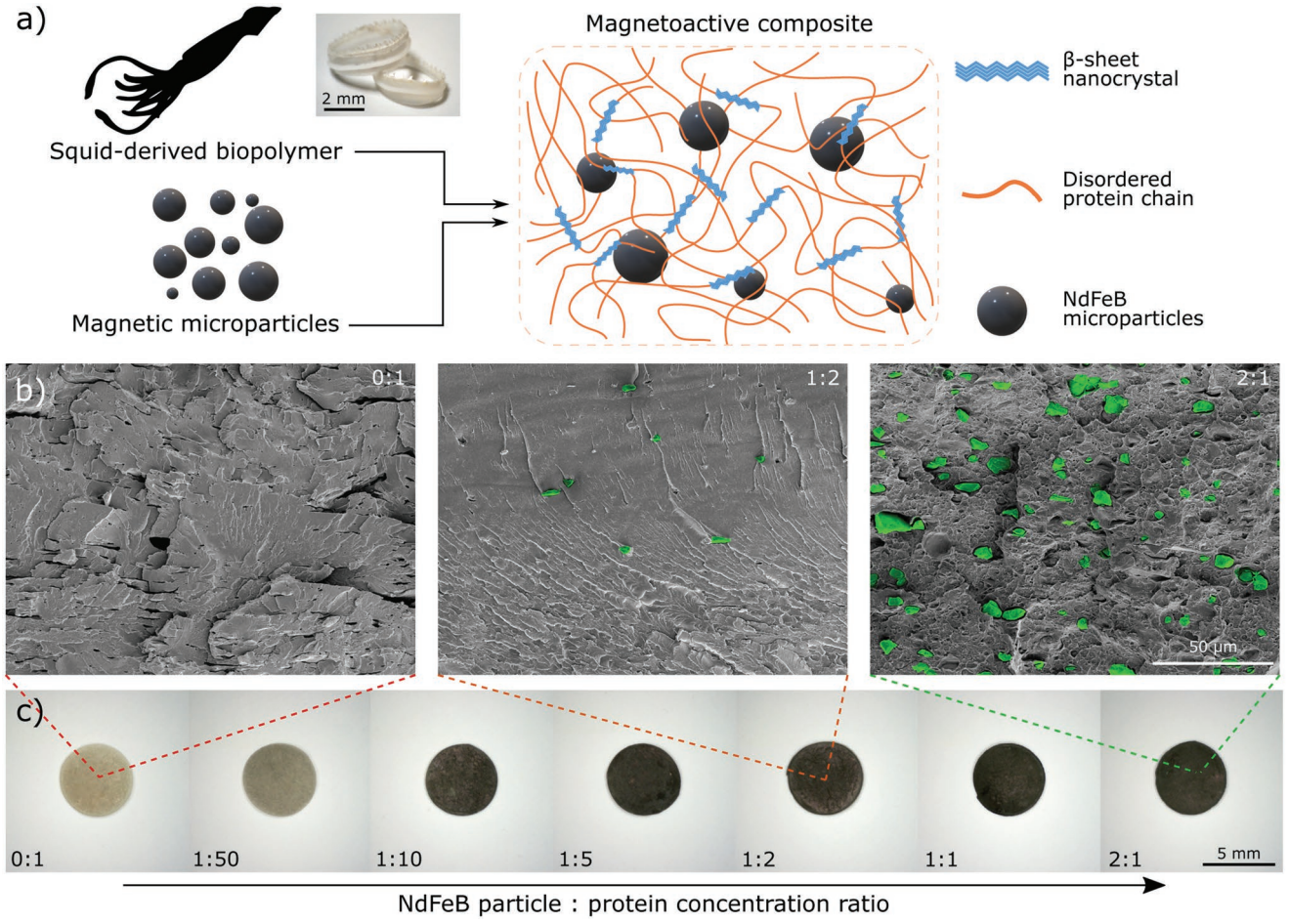

Figure 1. Fabrication of magnetoactive composites. a) NdFeB microparticles are dispersed in a squid-derived biopolymer matrix with semicrystalline morphology. b) SEM images of magnetoactive composites show good dispersion of NdFeB microparticles (colored in green). c) Composites with varying particle loading show a color change from white to black with increasing particle content.

© 2023 The Authors. Advanced Functional Materials published by Wiley-VCH GmbH

the network, constituting the amorphous phase of the semicrystalline structure and providing the material with shape-memory properties.[25,26] While SRT proteins have been explored in soft small-scale devices,[27–29] they present an excellent materials platform for the reconfigurable programming of modular magnetic actuators due to their dynamic structure and reversible properties.

Here, we develop protein-based composites from SRT proteins and NdFeB microparticles with tunable ferromagnetic and thermomechanical properties. By leveraging the reversible crosslinking structures in the biopolymer matrix, we developed a healing-assisted interfacial welding process that allows for the physical reconfiguration and magnetic reprogramming of anisotropic composites. We demonstrate this concept in multimaterial composite actuators with programmable deformations under homogeneous magnetic fields, with shape-memory behavior to lock in their preferred configuration. The actuators are healed after extreme mechanical damage (recovering their performance) and are reconfigured to different tasks and functions without the need for remagnetizing or demagnetizing. These dynamic magnetic soft composites can enable the modular design and assembly of new types of magnetic actuators, not only eliminating device vulnerabilities through healing and repair but also by providing adaptive mechanisms to reconfigure their function on demand.

2. Results and Discussion

2.1. Self-Healing Biopolymer Magnetic Composites

2.1.1. Design and Fabrication of Composites

Magnetic soft composites were fabricated by dispersing NdFeB microparticles in a structural protein network matrix (Figure 1a). NdFeB particles are commonly used in magnetic soft robotics due to their hard ferromagnetic behavior and high remanence (i.e., they maintain their magnetization at zero field).[7,9] The NdFeB microparticles used here are 5 μm in diameter, which is small enough to achieve good dispersion in the biopolymer matrix while large enough to exhibit ferromagnetic properties.[5] The biopolymer matrix is derived from sucker ring teeth (SRT) proteins derived from *Loligo vulgaris* squid species.[30] To fabricate the composites, SRT proteins were dissolved in hexafluoroisopropanol and NdFeB microparticles were added to the solution at the desired concentrations. Due to their size, NdFeB microparticles can sediment in the protein solution, which can result in their accumulation at the bottom of the container and a heterogeneous distribution. To avoid this issue, the solution was stirred before casting to facilitate the good dispersion of particles. NdFeB/protein solutions were cast into polydinethyl siloxane (PDMS) molds and the solvent was evaporated. The protein-particle composites exhibited good and uniform dispersion, with no visible aggregates or voids under scanning electron microscopy (Figure 1b). We prepared protein-particle composites with increasing particle concentration from 1:50 to 2:1 weight ratios (including control samples without particles, 0:1). As expected, the color of the composites changed from white to black with increasing particle content (Figure 1c). In all cases, we observed a homogeneous particle distribution in the bulk sample and did not observe any phase separation. To verify that the inclusion of particles does not disrupt the natural structure of the protein matrix, we characterized the protein nanostructure by Fourier transform infrared spectroscopy (FTIR). The FTIR spectra of the samples did not show any significant changes from the control (no particles) protein sample, with the major absorption bands characteristic of proteins shown at amide I (1600–1700 cm^{-1}), amide II (1510–1580 cm^{-1}), and amide A (3300 cm^{-1}) (Figure S1). Particularly, the amide I band, which corresponds to the carbonyl stretching vibration and contains information about the backbone hydrogen bonding and protein secondary structure, did not change with particle loading and showed a maximum at 1634 cm^{-1}, which corresponds to β-sheet nanostructures.[25,31] These results suggest that the protein nanostructure and β-sheet crosslinking nanocrystals are not disrupted by the inclusion of particles.

2.1.2. Characterization of Magnetic and Mechanical Properties

The actuation of soft materials with magnetic fields depends on the magnetic and mechanical properties since it involves competing magnetic force/torque (which depends on the material's magnetization) and the internal bending moment (which depends on the material's modulus).[32] Therefore, control over both the magnetic and mechanical properties is critical in the design of active materials for programmable actuation. The magnetic properties of the composites were characterized in a vibrating sample magnetometer (VSM), and their magnetic hysteresis loop is shown in **Figure 2**a. The composites exhibit clear ferromagnetic properties with large magnetic remanence and coercivity, which arise from the ferromagnetic NdFeB particles embedded in the protein matrix. The magnetization reaches saturation at ≈18 kOe in all samples. We measured the saturation magnetizations with increasing particle concentration up to 60 emu g^{-1} for the 2:1 composite (highest particle loading), which agrees with other reports of magnetic composites with similar particle loading ratios.[33] All samples exhibited high remanence (remaining magnetization when the external field is zero), which is characteristic of ferromagnetic materials and enables the programmable actuation of these composites. Since typical excitation magnetic fields for actuation are in the range of ≈10 mT (0.1 kOe), the working magnetic moment during actuation is enough to exploit the ferromagnetic properties of the composites and achieve the desired deformations.

To enable chain mobility in the protein network, the amorphous phase was plasticized with water. The plasticization of biopolymers is a known phenomenon that decreases the glass transition temperature (T_g) due to increased chain mobility, thus giving access to the rubbery state at lower temperatures than in dehydrated conditions.[26,34] The samples were hydrated in a submersion chamber during dynamic mechanical analysis (DMA) to measure both the glassy and rubbery states over a 15–70 °C temperature range (Figure 2b). The control protein samples without particles (0:1) exhibited a storage modulus of ≈1 GPa (glassy state) at low temperatures (15 °C). As the

© 2023 The Authors. Advanced Functional Materials published by Wiley-VCH GmbH

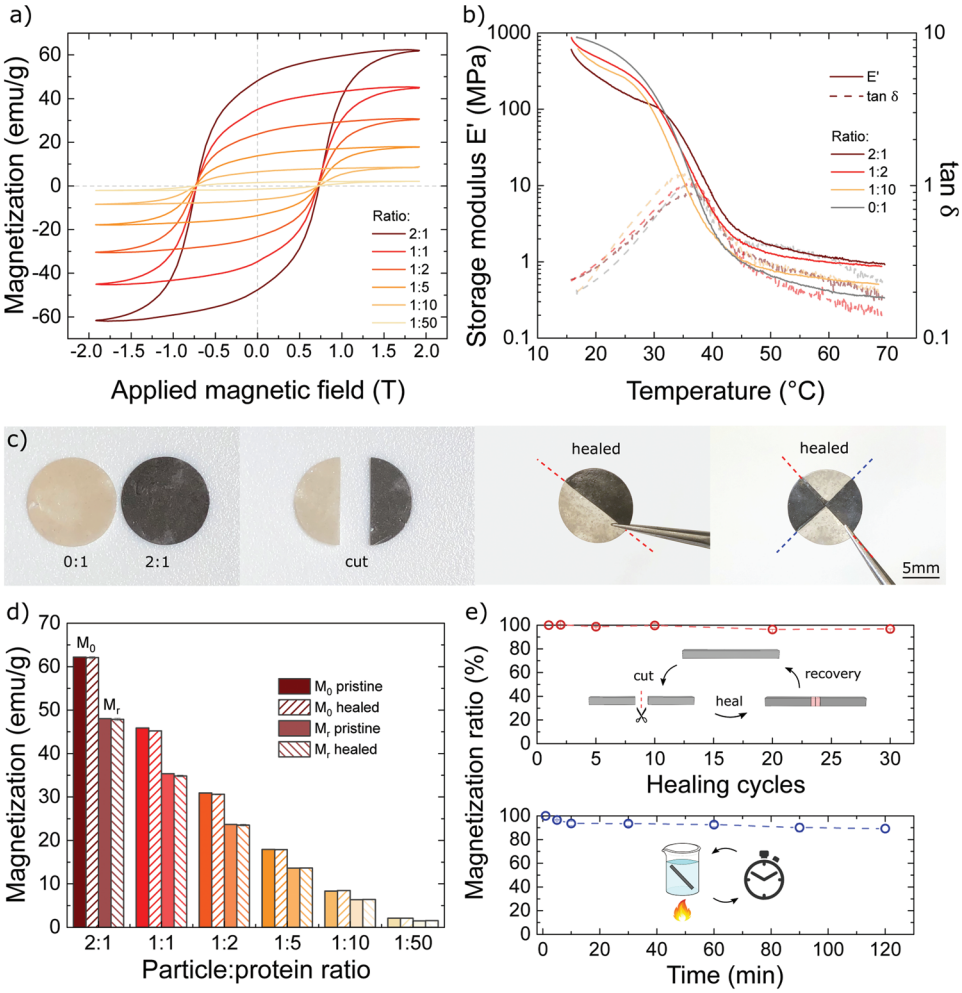

Figure 2. Magnetic, mechanical, and healing properties of magnetoactive composites. a) Magnetic characterization of composites, showing ferromagnetic behavior with remanence as a function of particle concentration. b) Mechanical characterization of composite with varying particle loading, showing a glass transition at 37 °C and a GPa to MPa change in modulus as a function of temperature. c) Composites with different particle loading are cut (mechanical damage) and healed at the interface multiple times. d) Magnetic properties are preserved after the self-healing process in all samples independently of particle concentration (M_0 and M_r are coercivity and remanence, respectively). e) Magnetization is maintained after multiple healing cycles and long-time healing cycles above the glass transition temperature (70 °C). Sample size for each measurement $n = 3$. Error bars represent one standard deviation.

temperature increases, the modulus progressively decreases until it plateaus at 1 MPa at 70 °C (rubbery state). This is due to a glass transition, observed at 37 °C as a peak in the tan delta. This behavior agrees with previous measurements of *Loligo vulgaris* SRT proteins.[35] As we incorporate magnetic particles in the protein matrix, the overall mechanical properties of the composites do not significantly differ from the protein control material, indicating that they are dominated by the protein matrix. Similar glass transition temperatures were observed at varying particle loading, indicating that the particles did not disrupt the protein structure and that the glass transition is primarily dependent on the protein matrix. At low temperatures, the moduli slightly decreased with higher particle concentrations, which is probably caused by the introduction of defects with the addition of particles. However, above the T_g (rubbery state), composites with higher particle loading consistently stiffen and exhibit a higher modulus, which is observed in particle-filled magnetic-responsive elastomers (MREs) and is expected within this particle range (particle volume fraction up to $\phi = 0.25$ for the composite series in this work).[5] These reversible properties give access to a wide range of moduli as a function of temperature (from GPa to MPa range), which will in turn determine the bending moment and overall performance of the actuators.

2.1.3. Healing Properties

The plasticization of the protein network increases the mobility of the chains in the amorphous phase, allowing for enhanced diffusion dynamics.[26] This not only results in the softening of the network (as measured by a decrease in modulus) but also in the emergence of healing properties. The protein network is stabilized by β-sheet nanocrystals as reversible physical crosslinks; however, these nanostructures cannot reform in the glassy state as the chains have limited mobility and

© 2023 The Authors. Advanced Functional Materials published by Wiley-VCH GmbH

are kinetically trapped.[18,26] Hence, no healing properties are observed below T_g or in the unplasticized (dehydrated) protein network. However, the increased diffusion above T_g (~40 °C) allows for enough diffusion to enable the healing of the network. This sharp healing dependence on temperature enables a controlled switching behavior that is critical and is a key differentiator from other self-healing matrices, as healing at room temperature can result in stickiness, undesired self-adhesion, and low modulus (limiting the work output of actuators).[36–38] The healing can be observed both in the control protein samples and in the magnetic composites (regardless of particle loading) since the thermomechanical properties are dominated by the protein matrix (as previously discussed). This is observed in Figure 2c, where 0:1 (no particles) and 2:1 (maximum loading) samples are cut and healed together multiple times. The two joined pieces exhibit clean interfaces, suggesting that there is no diffusion of particles from one part to the other. This process is performed by plasticizing the protein matrix with water at 45 °C and gently pressing the cut surfaces together to ensure good contact. This process is performed under a minute, including sample preparation, healing, and cooling, and can be performed multiple times without significant loss of structural and mechanical properties. IR spectroscopy on magnetic protein composites healed multiple times (i.e., cut into small pieces and thermally healed into a new sample) yielded overlapping spectra with no significant changes (Figure S2, Supporting Information). Similarly, DMA on samples healed over multiple cycles revealed the same thermomechanical properties with no significant loss (Figures S3and S4, Supporting Information).

The healing process occurs at temperatures much lower than the Curie temperature of NdFeB (> 300 °C), so loss of magnetic properties due to demagnetization is not expected. However, due to the softening of the protein matrix, particles could potentially rotate, diffuse, and misalign within the protein network, or leak from the material entirely. In order to assess the impact of the self-healing process on the magnetic properties, magnetic hysteresis loops were mapped before and after a healing cycle (Figure S5, Supporting Information). The measured saturation magnetizations and saturation remanences of composites with varying particle loading were compared in Figure 2d. The saturation magnetization and magnetic remanence for each sample composition were nearly identical before and after a healing cycle, with no observable loss of particles or properties. To expand the characterization beyond a single healing cycle, we measured the remanence after 30 healing cycles on the same sample without observing a significant loss (Figure 2e). Furthermore, we exposed the samples to the extreme conditions for healing over long exposure times (70 °C, which is higher than the healing temperature, and for up to 2 h of continuous thermal treatment), measuring remanences with less than 10% loss (which we believe is caused by repeated manipulation of the same sample and potential loss of material during loading/unloading in adhesive sample holders). Based on these results, we can conclude that the thermal cycling does not deteriorate the structural, mechanical, and magnetic properties of the protein-particle composites, and therefore it is a viable strategy for the processing, healing, and reconfiguration of the material.

2.2. Thermo-Responsive Magnetic Actuators

To program the response to magnetic stimuli and to achieve controlled bending actuation, we first wrote the magnetization of the particles in the composite. The particles were initially non-magnetized and randomly aligned within the soft matrix, and therefore did not have an initial coordinated magnetization. However, if exposed to a high-intensity homogeneous magnetic field in a specific direction, the magnetic moment of the particles will align with the external field (**Figure 3**a). Due to the ferromagnetic properties of NdFeB (high remanence), the new moment will be conserved when the external field is removed, thus resulting in programmable magnetization profiles. This strategy has been demonstrated in different anisotropic magnetization profiles in ferromagnetic composites for different bending actuation modes.[8] When exposed to a low-intensity actuation field, a given magnetization profile will generate magnetic torque over the soft composite body, which will in turn result in bending deformation. For example, a cantilever composite film magnetized through its thickness and exposed to a homogeneously magnetic field along the length direction will result in the bending of the film to align its moment with the external field (Figure 3b). This is shown for a protein composite cantilever beam magnetized horizontally (left to right) under a vertical field (upward) (Figure 3c). The beam rests vertically and flat (no bending) at zero field, but bends with increasing field due to the generated magnetic torque (to the left or the right with negative and positive fields respectively).

To characterize the bending actuation, we measured the cantilever tip displacement d (from its rest state) as a function of the actuation field (Figure 3d). At 20 °C, the actuator exhibits a linear dependence with the actuation field over a broad range of intensities due to the high modulus of the protein matrix. However, as temperature is increased, the protein matrix softens and becomes more flexible, exerting less resistance to the magnetic torque and enabling larger deformations. Therefore, the actuator becomes more sensitive to the field, with increased linear response and maximum displacement achieved at lower fields. By taking advantage of the reversible thermo-responsive mechanical properties of the protein matrix, we can tune the composite's modulus to the desired performance under the same field range. For example, one can reversibly switch between small deflections with low sensitivity to the field (low $\delta D/\delta B$) and large deflections with high sensitivity (high $\delta D/\delta B$) on demand. This behavior is also consistent with different composite formulations with varying particle loading, which have different remanence and sensitivity to the actuation field ($\delta D/\delta B$) (Figure 3e; Figure S6, Supporting Information). Therefore, this protein-particle composite materials system allows for the full tunability of the actuator's performance by: i) formulating particle loading for the desired remanence, ii) programming the bending mode by writing an anisotropic magnetization profile, iii) controlling the temperature for tuning sensitivity and switching modes, and iv) controlling the external actuation field for bending control.

In addition, the healing properties of the protein matrix can enable the repair and recovery of function after the actuator is damaged. As previously discussed, the healing process does not deteriorate the mechanical or magnetic properties of the

© 2023 The Authors. Advanced Functional Materials published by Wiley-VCH GmbH

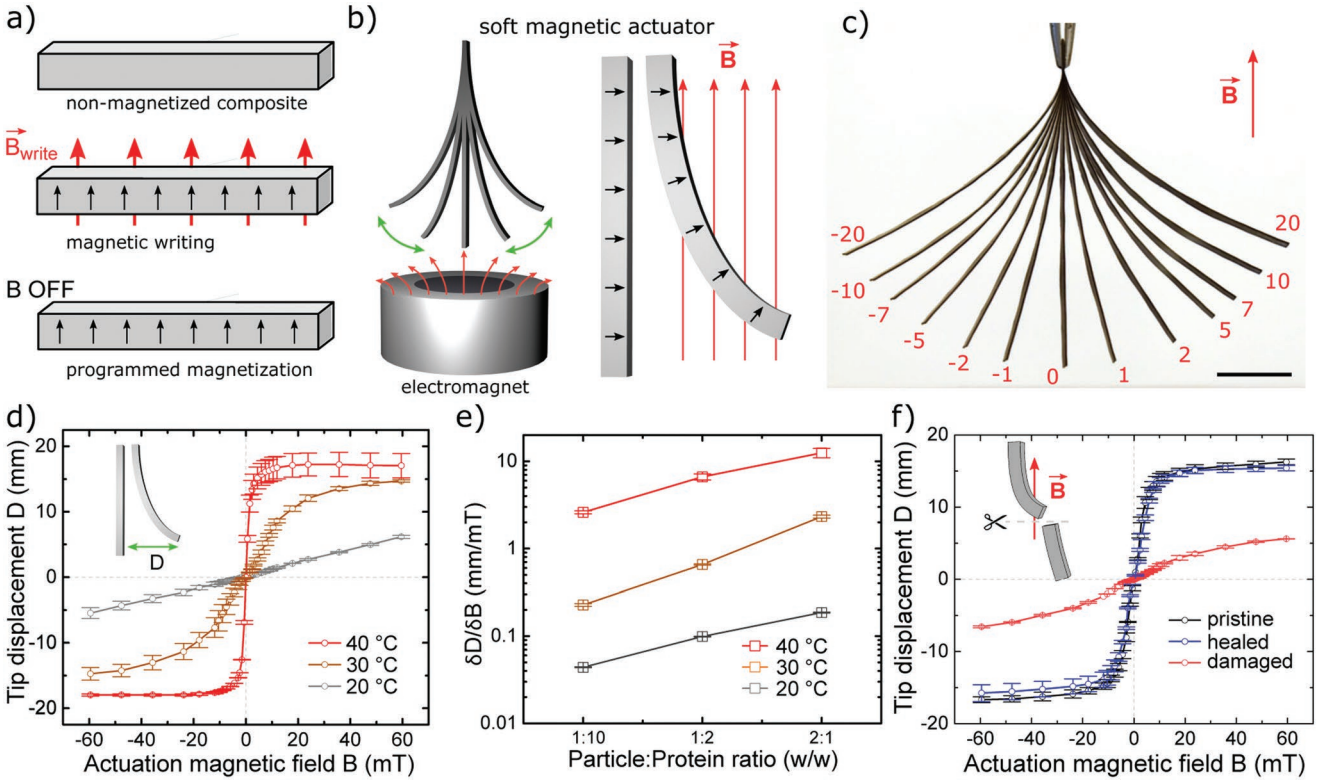

Figure 3. Magnetic soft actuator. a) Composites are magnetized under a high-intensity writing magnetic field in a specified direction. b) Soft magnetic actuator bends due to torque generated from a magnetic field (vertical) and the internal composite magnetization (horizontal, perpendicular to field), leading to left/right tip displacement. c) Bending and tip displacement of the soft actuator (2:1 particle: protein ratio) under an upward actuation field (unit numbers: mT; scale bar: 5 mm). d) Actuator tip displacement as a function of actuation magnetic field and temperature, exhibiting thermoresponsive field sensitivity. e) Sensitivity to field ($\delta D/\delta B$) as a function of temperature and particle loading. f) Tip displacement of a pristine, damaged (cut), and healed actuator (2:1 particle: protein ratio, 40 °C), showing a loss of displacement after damage and recovery after healing. Sample size for each measurement $n = 3$. Error bars represent one standard deviation.

composite, including the internal anisotropic magnetization profile. In Figure 3f we measured the tip displacement D of an actuator as a function of varying magnetic fields. We then cut the beam to simulate mechanical damage and detachment, and observed a significant performance loss: drop in $\delta D/\delta B$ sensitivity in the linear region, lower plateau at high field, and loss in maximum displacement (caused by the loss of material and reduction in length of the actuator). However, when the detached piece is healed back into the beam structure, no distinguishable performance difference is observed between the pristine and healed actuators (within experimental error of each other). Therefore, the actuators can be healed and the performance recovered after damage that would otherwise terminate the device function, improving the overall durability of soft magnetic actuators and enabling their resilience to mechanical damage.

2.3. Reconfigurable Modular Actuators with Discretized Magnetization

The dynamic nanostructure of SRT proteins enables the healing and recovery of properties and performance of magnetic actuators; however, it can also enable new functions and designs via modular assembly and reconfiguration of actuator components. For example, magnetic SRT composite and non-magnetic SRT materials can be joined together and healed at the interface, yielding continuous protein materials with inhomogeneous composition and discretized magnetization (**Figure 4**a). This multimaterial approach has the main advantage that magnetic torques can be localized in the magnetic components only. The non-responsive, non-magnetic components are more compliant and will still bend to accommodate the torque on the magnetic components. However, due to the lower modulus (non-magnetic component) and the localized torque (magnetic torque), the actuator can achieve similar bending angles than its homogeneous analogous at lower tip displacements and larger curvatures (Figure 4b; Figure S7, Supporting Information), which gives access to operation in smaller confined spaces. Furthermore, this approach gives access to new actuator designs by its modular assembly and reconfiguration. Modularity in soft magnetic actuators has been recently explored by assembling multiple magnetized soft components with discretized magnetization, providing access to complex discretized magnetization profiles that are difficult to achieve otherwise under a homogeneous magnetizing field. However, once assembled, these discretized magnetization profiles are permanent, thus limiting their use to a single design and actuation mode. Dynamically crosslinked materials such

© 2023 The Authors. Advanced Functional Materials published by Wiley-VCH GmbH

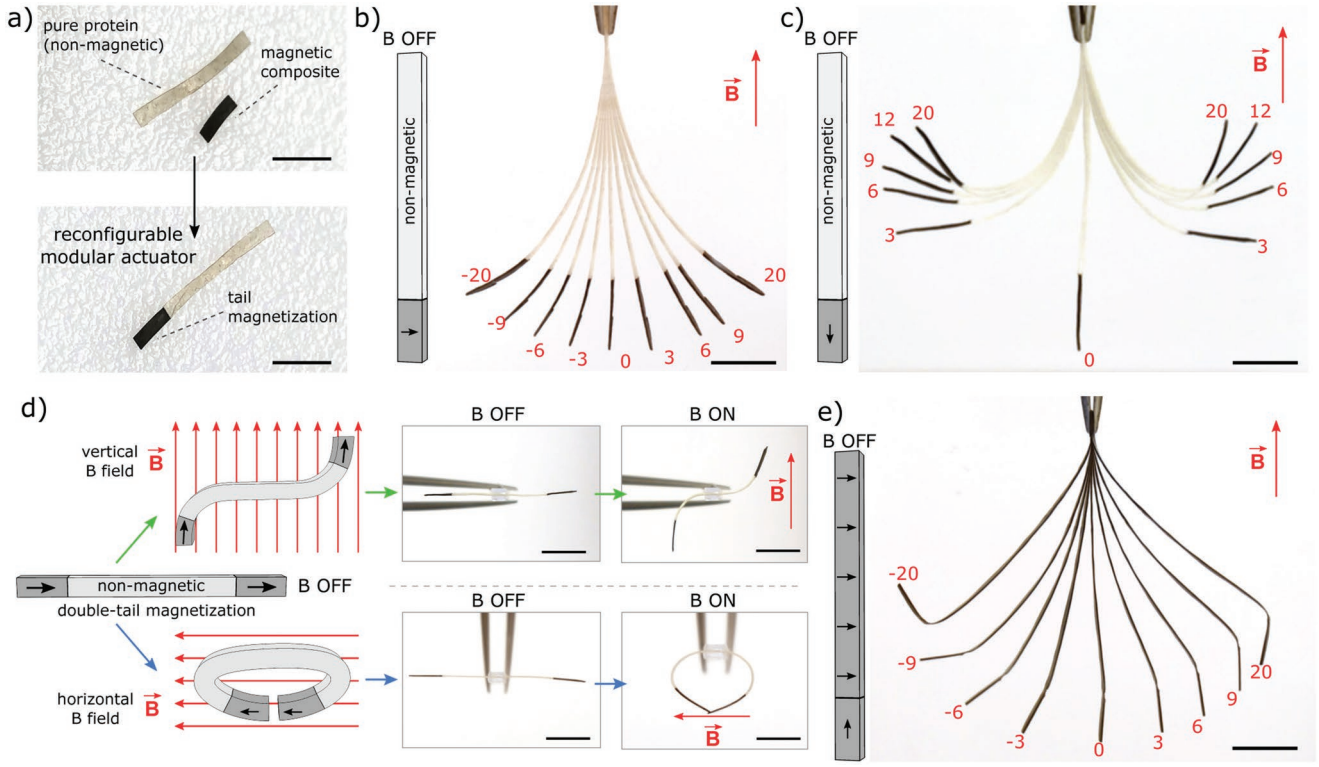

Figure 4. Modular assembly of multimaterial and discretized soft magnetic actuators (2:1 particle: protein ratio, actuated at 40 °C in a water bath). a) Magnetic actuators fabricated by combining modular composite materials with desired magnetic properties and geometries via interfacial healing. b) Multimaterial actuator with a non-magnetic protein core and a magnetized tail (right-magnetized) under a vertical field. c) Multimaterial actuator with a non-magnetic protein core and a magnetized tail (down-magnetized) under a vertical field. d) Multimaterial actuator with a non-magnetic protein core and a magnetized double tail under a vertical and horizontal field. e) Multimaterial discretized actuator with discretized magnetization, with a right-magnetized core and an up-magnetized tail under a vertical field.

as SRT enable the reconfiguration of discretized magnetization profiles by removing or adding components to the actuator without loss of properties or material. For example, an actuator strip with tail magnetization had its tail removed ("right" magnetization, Figure 4b) and replaced with a tail of the same dimensions but with different magnetization ("down" magnetization, Figure 4c). This modular reconfiguration resulted in a new actuation mode that was previously inaccessible under the same external field: due to the reconfigured magnetization, the external field generates greater magnetic torque to bend the tip up, leading to a higher curvature at the joint at small displacements, providing a larger and tunable deformation range.

This healing assembly approach allows for the incorporation of multiple discretized, interchangeable magnetic components, and therefore expands the actuator design space to many modular configurations. For example, two magnetized components (magnetized parallel to the strip) were assembled at the ends of a non-magnetic protein actuator via interfacial healing, resulting in double-tail magnetization (Figure 4d). The double-tail configuration combines the coordinated torque-driven actuation of the magnetized ends with the flexibility of the central soft protein core, thus resulting in high curvature bending at the softcore. This can be observed when an external magnetic field is applied perpendicularly to the strip and magnetization directions, resulting in the upwards and downward bending of the softcore. Similarly, when the field is applied parallel but opposed to the magnetization direction, the actuator bends downward with high curvature in the softcore. This discretized modular design can achieve high curvatures in the soft cores and achieve high bending in confined spaces, and can be extended to many designs with multiple functional components with tunable stiffness, degree of magnetization, and direction of magnetization. For example, multiple magnetization profiles can be combined into a single actuator (Figure 4e). In this case, a composite protein actuator was designed and assembled with the core and tail magnetized perpendicular and parallel to the strip directions respectively. Under the same homogeneous actuation field, this modular profile results in torques distributed heterogeneously throughout the soft composite volume and therefore results in complex bending modes derived from the discretized design. This versatile modular design approach of continuous, monolithic actuators with discretized, reconfigurable components allows for magnetization profiles and configurations that cannot be achieved with continuous magnetization methods, with the additional main advantage that they can be reconfigured (i.e., dismantled, recombined, ad re-assembled) on demand and for an unlimited number of cycles due to the soft-core healing properties. The presented modular actuators have been assembled manually, with is sufficient for simple designs and low number of components. However, manual assembly will eventually limit the throughput of the manufacturing method and limit the

© 2023 The Authors. Advanced Functional Materials published by Wiley-VCH GmbH

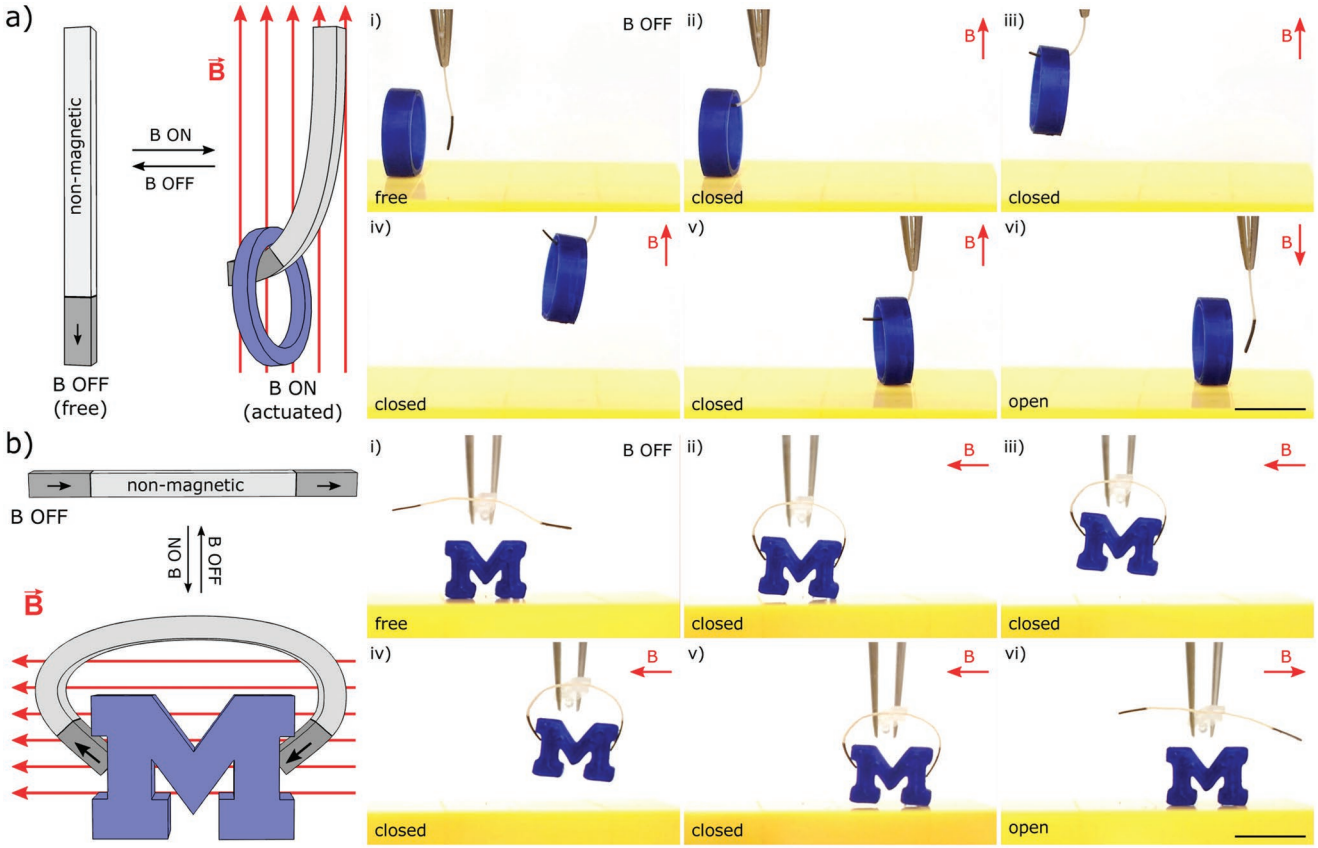

Figure 5. Multimaterial modular soft grippers. a) Cantilever actuator with a soft protein core and tail magnetization for bending and transportation of a ring-shaped payload. b) Cantilever actuator with a soft protein core and double-tail magnetization for coordinated bending and compliant grasping of payload with complex geometry. Scale bar: 10 mm.

complexity and number of components in the actuators. An advanced modular manufacturing system would enable the fabrication of high-complexity actuators through a digital automated design.

2.4. Magnetic Shape-Memory Soft Grippers with Catch/Release States

In this section, we leverage the control over the reversible thermo-responsive, magnetization, and modular reconfiguration properties of the protein magnetic composites to design soft actuators for specific gripper functions and to implement them in small-scale manipulation prototypes. In short, the actuator must be able to perform three sequential functions in a pick-and-place task: grasping the payload, holding the payload (lift and travel during transportation), and releasing the payload at the destination. A model actuator design is a single-cantilever actuator with a nonmagnetic soft protein core and a magnetic composite tail (magnetized along the axis) (**Figure 5**a; Movie S1, Supporting Information). Upon actuation, the magnetic tail aligns with the external field, generating torque and bending on the soft protein core of the actuator. The bending deformation results in a reversible transition into a "hook" shape that can grasp and hold hollow objects (such as the ring-shaped object). A second model design is a dual-cantilever actuator also with a nonmagnetic soft protein core and a magnetic composite double-tail (magnetized along the axis in the same direction) (Figure 5b; Movie S2, Supporting Information). When a homogeneous horizontal magnetic field is applied, the torque generated at the tails bends the soft actuator arms inward, resulting in coordinated and opposing deformation to grasp and hold an object. Due to the softness of the protein matrix, the arms of the actuator can conform and adapt to complex geometries of the payload, leading to higher contact area and better grasping. In both cases, small actuation fields (20 mT) are sufficient to bend the composite modular actuators to effectively grasp the payload, hold its weight during transportation, and release it on demand in pick-and-place tasks.

One common limitation of magnetic actuators is that they require a constant excitation field in order to keep the actuator in its activated state and keep the applied force/torque. When the field is turned off, the applied forces/torques are removed and the actuator is deactivated (immediately releasing the cargo). Therefore, constant field (and in electromagnets, constant current) is required to keep the actuator in an active "hold" or "catch" state, which is extremely inefficient and can quickly lead to coil overheating. These limitations can be overcome with the use of the SRT dynamic protein matrix due to its reversible thermomechanical properties. As previously described, the protein matrix has a temperature-responsive modulus with a glass transition temperature T_g at 37 °C. Above

© 2023 The Authors. Advanced Functional Materials published by Wiley-VCH GmbH

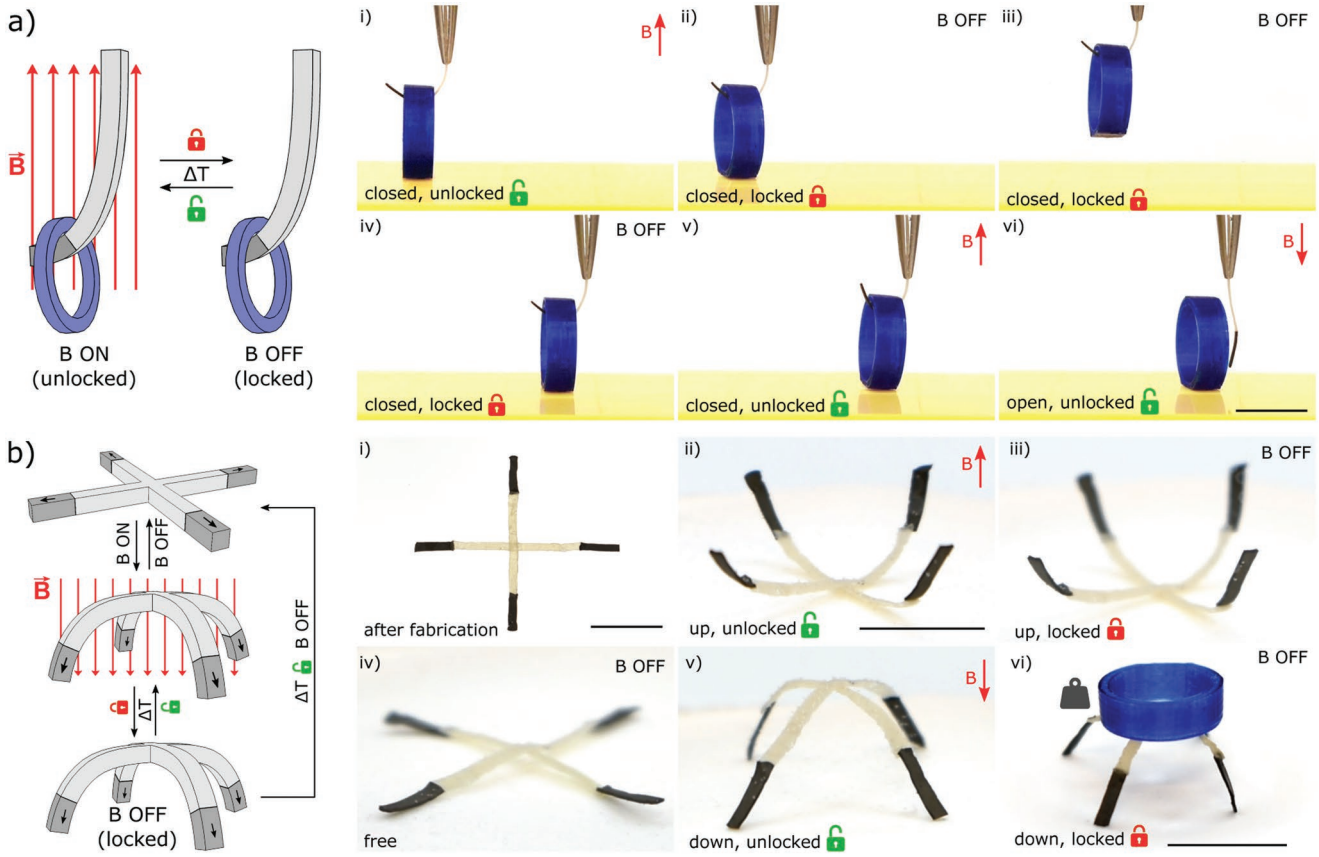

Figure 6. Shape-memory actuators for lock-in states. a) Single-cantilever actuator with tail magnetization. Temperature control is used to reversibly tune the stiffness of the actuator, locking its shape and achieving a locked catch state without the need for actuation field. b) 4-arm actuator with tail magnetization and reversible concave/convex bending. Actuated states are locked-in with temperature control, and are preserved after removing the actuation field and under load. Scale bars: 10 mm.

the T_g, the actuator can bend with the external magnetic field, or relax back to the original state when the field is removed. However, below T_g, the protein matrix has higher modulus and stiffness, which limits the deformation. By alternating the temperature between these two states, we can deform the actuator at $T > T_g$ to its desired shape using magnetic fields, and then lock its shape at $T < T_g$. When locked, the actuator keeps its shape and activated "catch" state after the field is removed, thus exhibiting a shape-memory behavior that can be exploited for soft gripping applications. Due to the high sensitivity to temperature of the actuators, a water bath is used to ensure a homogeneous temperature in the environment. However, due to the thermal mass of the bath, the changes in temperature are slow. This could be further optimized for specific applications with faster heating/cooling kinetics using other heating methods (induction, resistive, photothermal, etc.).

This shape-memory locking approach is tested in the single-cantilever "hook" actuator by homogeneously controlling the temperature of a water bath (**Figure 6**a). After applying the actuation magnetic field to bend the actuator into the desired shape (grasping the ring payload), we can decrease the temperature and lock it in the activated "catch" state. This "catch" state is maintained after the removal of the external magnetic field, without any energy input to hold the payload and transport it to its desired position. When the payload reached its target final position, we can increase the temperature, soften the actuator, and apply magnetic fields to release the payload (Movie S3, Supporting Information). This concept can be applied to shape-memory transformations beyond gripping to achieve complex deformations and switching behavior between transient and permanent transformations.[39,40] A free 4-arm actuator with a protein softcore and tail magnetization on each arm was used to demonstrate this approach (Figure 6b). At $T > T_g$,, positive/negative excitation fields were applied to achieve reversible concave/convex shape transformations (Movie S4, Supporting Information). However, at $T < T_g$, we can lock the actuator in its desired shape. Further switching between positive/negative fields doesn't disrupt the shape due to the high stiffness of the protein matrix at $T < T_g$ temperatures (actuator arms do not bend, but the whole assembly rotates with the applied field instead). In the locked configuration, the 4-arm actuator can hold the weight of the same cargo without any external field and without any visible deformation or disruption.

3. Conclusion

We have designed a magnetic soft composite consisting of ferromagnetic particles dispersed in a squid-derived biopolymer matrix with dynamic properties. While NdFeB microparticles

© 2023 The Authors. Advanced Functional Materials published by Wiley-VCH GmbH

provide a way to program the internal magnetization of the composite due to their remanence, SRT proteins provide adaptive properties due to the stimuli-responsive semicrystalline protein nanostructure. On one hand, nanocrystalline β-sheets provide a hydrogen-bond-stabilized, reversible crosslinking mechanism that can be used to repair the protein network from mechanical damage across multiple length scales. On the other hand, the amorphous protein phase has a glass transition temperature at $T_g = 37$ °C that provides temperature-responsive mechanical properties through a glassy-to-rubbery transition. Combined together, the dynamic properties of this composite materials system open the design space of magnetic soft actuators by enabling their reversible modular assembly, their reconfiguration, and reprogramming for adaptation to multiple tasks on demand, and their repair after severe mechanical damage (recovering their function after loss). We have demonstrated these properties and unique features in a set of multi-smaterial composite actuators with programmable deformations under homogeneous magnetic fields, with thermo-responsive shape-memory behavior to lock in their preferred configuration and to achieve catch states without energy consumption. The dynamic magnetic soft composites developed in this work can enable the modular design and assembly of new types of magnetic actuators, not only eliminating device vulnerabilities through healing and repair but also by providing new adaptive mechanisms to reconfigure their function on demand without the need for remagnetizing or demagnetizing. While the control systems external to the material can be further optimized (for example, for better temperature control and faster heating rates), the materials characterization and actuator prototypes described in this work highlight the versatility and potential of protein-based materials as a programmable platform to design adaptive systems.

4. Experimental Section

Materials Fabrication: Squid ring teeth (SRT) were obtained from the tentacles of the *Loligo vulgaris* squid from Tarragona, Spain. SRT protein was dissolved in hexafluoroisopropanol (HFIP, Sigma Aldrich #1 05 228) at a concentration of 50 mg ml^{-1}. The protein solution was then mixed with ferromagnetic microparticles (NdFeB, Magnequench MQFP-15-7-D50) at specific protein-to-particle mass ratios to form composite pre-suspension. The suspension was thoroughly mixed to avoid particle sedimentation. SRT/HFIP/NdFeB (100 µL) were cast on PDMS substrates and left to evaporate in the fme hood to obtain the magnetic composite strips.

Scanning Electron Microscopy (SEM): Samples were coated with a gold film (10–20 nm) in an SPI-Module Sputter Coater and imaged on the Thermo Fisher Nova 200 Nanolab SEM.

IR Spectroscopy: Protein nanostructures were analyzed using Fourier transform infrared spectroscopy (FTIR) in a ThermoFisher Nicolet iS20 spectrometer with a platinum ATR accessory. The FTIR spectra were performed with 128 scans at 4 cm^{-1} resolution, and were baseline-corrected and normalized to the amide I band at ≈1630 cm^{-1}.

Mechanical Characterization: Composite samples were fabricated into strips with 100 µm thickness through self-healing and were hydrated in water for at least 1 h before the test. Samples were characterized in a TA Instruments Discovery DMA 850. Samples were mounted in a submersion film clamp and were measured in water media at 1 Hz and a 3 µm amplitude. The temperature swept from 10 to 70 °C with a heating ramp speed of 2 °C min^{-1}.

Magnetic Characterization: The magnetic properties of the SRT/NdFeB composites were characterized at room temperature in a Lake Shore 7400 vibrating sample magnetometer (VSM). Magnetic hysteresis loops were acquired using a scanning field within the range of ±18 kOe, and were normalized by the sample weight. VSM was later utilized to test the impact of healing cycles and healing time on the samples' magnetization. After specified healing cycles and/or healing time (70 °C), the samples were mounted to the VSM, and their magnetizations were measured at zero external fields.

Sample Magnetization: The composite samples were magnetized under a 1.5 T external magnetic field generated from VSM in a direction parallel or perpendicular to composite samples to generate in-plane or out-of-plane magnetic moments.

Healing of Composites: SRT/NdFeB samples were cut using a razor blade into predetermined geometries with straight edges. Composite pieces were aligned by the edges and placed between two PDMS films for support. The samples were hydrated with DI water and heated to 70 °C for 1 min under gentle pressure until they heal into a single piece. Samples were cooled down in ambient conditions.

Magnetic Actuation: The composite samples were immersed in a water bath with a set temperature and exposed to a magnetic field generated from an electromagnet (Bunting BDE-4032-12, with a DC power supply Tekpower TP3005P) spanning ± 60 mT. A Nikon camera (D3500) was used to record the actuation states, and the images were later analyzed using ImageJ (version: 1.8).

Supporting Information

Supporting Information is available from the Wiley Online Library or from the author.

Acknowledgements

Z.Z. and A.P.F thank the Seeding To Accelerate Research Themes (START) Program from the College of Engineering at the University of Michigan, and the American Chemical Society Petroleum Research Fund for partial financial support. J.T.H. acknowledges support from NSF CAREER grant DMR-1847847. The authors thank Prof. Jovan Kamcev for access to dynamic mechanical analysis instrumentation. All authors contributed to writing, data analysis, figure preparation, and revising of the manuscript and agreed on the final content.

Conflict of Interest

The authors declare no conflict of interest.

Data Availability Statement

The data that support the findings of this study are available in the supplementary material of this article.

Keywords

magnetic actuators, magnetoactive, modular assembly, protein biopolymers, reconfigurable structures, self-healing, shape-memory

Received: December 31, 2022
Revised: February 28, 2023
Published online: March 27, 2023

© 2023 The Authors. Advanced Functional Materials published by Wiley-VCH GmbH

[1] M. Li, A. Pal, A. Aghakhani, A. Pena-Francesch, M. Sitti, *Nat. Rev. Mater.* **2022**, *7*, 235.
[2] L. Hines, K. Petersen, G. Z. Lum, M. Sitti, *Adv. Mater.* **2017**, *29*, 1603483.
[3] Y. Kim, E. Genevriere, P. Harker, J. Choe, M. Balicki, R. W. Regenhardt, J. E. Vranic, A. A. Dmytriw, A. B. Patel, X. Zhao, *Sci. Robot.* **2022**, *7*, eabg9907.
[4] E. T. Roche, M. A. Horvath, I. Wamala, A. Alazmani, S.-E. Song, W. Whyte, Z. Machaidze, C. J. Payne, J. C. Weaver, G. Fishbein, J. Kuebler, N. V. Vasilyev, D. J. Mooney, F. A. Pigula, C. J. Walsh, *Sci. Transl. Med.* **2017**, *9*, eaaf3925.
[5] Y. Kim, X. Zhao, *Chem. Rev.* **2022**, *122*, 5317.
[6] K. Cerdan, C. Moya, P. Van Puyvelde, G. Bruylants, J. Brancart, *Molecules* **2022**, *27*, 3796.
[7] W. Hu, G. Z. Lum, M. Mastrangeli, M. Sitti, *Nature* **2018**, *554*, 81.
[8] G. Z. Lum, Z. Ye, X. Dong, H. Marvi, O. Erin, W. Hu, M. Sitti, *Proc. Natl. Acad. Sci. USA* **2016**, *113*, E6007.
[9] Y. Kim, H. Yuk, R. Zhao, S. A. Chester, X. Zhao, *Nature* **2018**, *558*, 274.
[10] T. Xu, J. Zhang, M. Salehizadeh, O. Onaizah, E. Diller, *Sci. Robot.* **2019**, *4*, aav4494.
[11] H.-W. Huang, M. S. Sakar, A. J. Petruska, S. Pané, B. J. Nelson, *Nat. Commun.* **2016**, *7*, 12263.
[12] J. Zhang, Z. Ren, W. Hu, R. H. Soon, I. C. Yasa, Z. Liu, M. Sitti, *Sci Robot.* **2021**, *6*, abf0112.
[13] Y. Dong, L. Wang, N. Xia, Z. Yang, C. Zhang, C. Pan, D. Jin, J. Zhang, C. Majidi, L. Zhang, *Sci. Adv.* **2022**, *8*, abn8932.
[14] Y. Alapan, A. C. Karacakol, S. N. Guzelhan, I. Isik, M. Sitti, *Sci. Adv.* **2020**, *6*, abc6414.
[15] X. Yang, R. Tan, H. Lu, T. Fukuda, Y. Shen, *Nat. Commun.* **2022**, *13*, 4156.
[16] S. Wang, M. W. Urban, *Nat. Rev. Mater.* **2020**, *5*, 562.
[17] B. J. Blaiszik, S. L. B. Kramer, S. C. Olugebefola, J. S. Moore, N. R. Sottos, S. R. White, *Annu. Rev. Mater. Res.* **2010**, *40*, 179.
[18] A. Pena-Francesch, H. Jung, M. C. Demirel, M. Sitti, *Nat. Mater.* **2020**, *19*, 1230.
[19] Y. J. Tan, G. J. Susanto, H. P. Anwar Ali, B. C. K. Tee, *Adv. Mater.* **2021**, *33*, 2002800.
[20] S. Terryn, J. Langenbach, E. Roels, J. Brancart, C. Bakkali-Hassani, Q.-A. Poutrel, A. Georgopoulou, T. G. Thuruthel, A. Safaei, P. Ferrentino, T. Sebastian, S. Norvez, F. Iida, A. W. Bosman, F. Tournilhac, F. Clemens, G. Van Assche, B. Vanderborght, *Mater. Today* **2021**, *47*, 187.
[21] A. Miserez, J. C. Weaver, P. B. Pedersen, T. Schneeberk, R. T. Hanlon, D. Kisailus, H. Birkedal, *Adv. Mater.* **2009**, *21*, 401.
[22] A. Pena-Francesch, M. C. Demirel, *Front. Chem.* **2019**, *7*, 69.
[23] P. A. Guerette, S. Hoon, Y. Seow, M. Raida, A. Masic, F. T. Wong, V. H. B. Ho, K. W. Kong, M. C. Demirel, A. Pena-Francesch, S. Amini, G. Z. Tay, D. Ding, A. Miserez, *Nat. Biotechnol.* **2013**, *31*, 908.
[24] H. Jung, A. Pena-Francesch, A. Saadat, A. Sebastian, D. H. Kim, R. F. Hamilton, I. Albert, B. D. Allen, M. C. Demirel, *Proc. Natl. Acad. Sci. USA* **2016**, *113*, 6478.
[25] A. Pena-Francesch, H. Jung, M. Segad, R. H. Colby, B. D. Allen, M. C. Demirel, *ACS Biomater. Sci. Eng.* **2018**, *4*, 884.
[26] A. Pena-Francesch, H. Jung, M. Tyagi, M. C. Demirel, *Biomacromolecules* **2022**, *23*, 3165.
[27] C.-H. Lin, C. Kinane, Z. Zhang, A. Pena-Francesch, *ACS Appl. Mater. Interfaces* **2022**, *14*, 39332.
[28] A. Pena-Francesch, J. Giltinan, M. Sitti, *Nat. Commun.* **2019**, *10*, 3188.
[29] N. P. Pinchin, C.-H. Lin, C. A. Kinane, N. Yamada, A. Pena-Francesch, H. Shahsavan, *Soft Matter* **2022**, *18*, 8063.
[30] A. Pena-Francesch, S. Florez, H. Jung, A. Sebastian, I. Albert, W. Curtis, M. C. Demirel, *Adv. Funct. Mater.* **2014**, *24*, 7401.
[31] X. Hu, D. Kaplan, P. Cebe, *Macromolecules* **2006**, *39*, 6161.
[32] L. Wang, Y. Kim, C. F. Guo, X. Zhao, *J. Mech. Phys. Solids* **2020**, *142*, 104045.
[33] J. Zhang, Y. Guo, W. Hu, R. H. Soon, Z. S. Davidson, M. Sitti, *Adv. Mater.* **2021**, *33*, 2006191.
[34] R. G. M. van der Sman, *Food Hydrocolloids* **2012**, *27*, 529.
[35] A. Pena-Francesch, B. Akgun, A. Miserez, W. Zhu, H. Gao, M. C. Demirel, *Adv. Funct. Mater.* **2014**, *24*, 6227.
[36] Y. Cheng, K. H. Chan, X. Wang, T. Ding, T. Li, C. Zhang, W. Lu, Y. Zhou, G. W. Ho, *Adv Funct Mater.* **2021**, *31*, 2101825.
[37] G. Dong, Q. He, S. Cai, *Soft Matter* **2022**, *18*, 7604.
[38] H. Tao, D. Yue, C. Li, *Macro Mater. Eng.* **2022**, *307*, 2100649.
[39] Q. Ze, X. Kuang, S. Wu, J. Wong, S. M. Montgomery, R. Zhang, J. M. Kovitz, F. Yang, H. J. Qi, R. Zhao, *Adv. Mater.* **2020**, *32*, 1906657.
[40] K. Yu, K. K. Westbrook, P. H. Kao, J. Leng, H. J. Qi, *J. Compos. Mater.* **2013**, *47*, 51.

© 2023 The Authors. Advanced Functional Materials published by Wiley-VCH GmbH